cisplatin plus pemetrexed in chemotherapy-naïve patients with advanced-stage non-small-cell lung cancer. J Clin Oncol 26 : 3543-3551, 2008
6) Sandler A, Gray R, Perry MC, et al : Paclitaxel-carboplatin alone or with bevacizumab for non-small cell lung cancer. N Engl J Med 355 : 2542-2550, 2006
7) Mitsudomi T : Advances in target therapy for lung cancer. Jpn J Clin Oncol 40 : 101-106, 2010
8) Weinstein IB : Disorders in cell circuitry during multistage carcinogenesis : the role of homeostasis. Carcinogenesis 21 : 857-864, 2000
9) Tanaka, T, Matsuoka H, Sutani A, et al : Frequency of and variables associated with the EGFR mutation and its subtypes. Int J Cancer 126 : 651-655, 2010
10) Sordella R, Bell DW, Haber DA, Settleman J : Gefitinib-sensitizing EGFR mutations in lung cancer activate anti-apoptotic pathways. Science 305 : 1163-1167, 2004
11) Maemondo M, Inoue A, Kobayashi K, et al : Gefitinib or chemotherapy for non-small-cell lung cancer with mutated EGFR. N Engl J Med 362 : 2380-2388, 2010
12) Mitsudomi T, Morita S, Yatabe Y, et al : Gefitinib versus cisplatin plus docetaxel in patients with non-small-cell lung cancer harbouring mutations of the epidermal growth factor receptor (WJTOG3405) : an open label, randomised phase 3 trial. Lancet Oncol 11 : 121-128, 2009
13) Ohe Y, Ohashi Y, Kubota K, et al : Randomized phase Ⅲ study of cisplatin plus irinotecan versus carboplatin plus paclitaxel, cisplatin plus gemcitabine, and cisplatin plus vinorelbine for advanced non-small-cell lung cancer : Four-Arm Cooperative Study in Japan. Ann Oncol 18 : 317-323, 2007
14) Engelman JA, Chen L, Tan X, et al : Effective use of PI3K and MEK inhibitors to treat mutant Kras G12D and PIK3CA H1047R murine lung cancers. Nat Med 14 : 1351-1356, 2008
15) Grieco M, Cerrato A, Santoro M, et al : Cloning and characterization of H4 (D10S170), a gene involved in RET rearrangements *in vivo*. Oncogene 9 : 2531-2535, 1994
16) Soda M, Choi : YL, Enomoto M, et al : Identification of the transforming EML4-ALK fusion gene in non-small-cell lung cancer. Nature 448 : 561-566, 2007
17) Takeuchi K, Choi YL, Soda M, et al : Multiplex reverse transcription-PCR screening for EML4-ALK fusion transcripts. Clin Cancer Res 14 : 6618-6624, 2008
18) Osoegawa A, Nosaki K, Miyamoto H : Incidentally proven pulmonary "ALKoma". Intern Med 49 : 603-606, 2010
19) Bang Y, Kwak EL, Shaw AT, et al : Clinical activity of the oral ALK inhibitor PF-02341066 in ALK-positive patients with non-small cell lung cancer (NSCLC). J Clin Oncol 28 (suppl ; abstr 3) : 18s, 2010

原著

携帯型インフューザーポンプを使用した5-FU持続投与コンプライアンスの調査

佐藤 淳也[*1,2] 照井 一史[*1,2] 粟津 朱美[*2] 小山 基[*3] 伊東 重豪[*2,4]
西條 康夫[*2,4] 早狩 誠[*1]

〔*Jpn J Cancer Chemother* 37(4): 671-675, *April*, 2010〕

Survey on the Compliance of Patients with Continuous Infusion of 5-Fluorouracil via Portable Infusion Pumps:

Junya Sato[*1,2], Kazufumi Terui[*1,2], Akemi Awatsu[*2], Motoi Koyama[*3], Jugoh Itoh[*2,4], Yasuo Saijo[*2,4] and Makoto Hayakari[*1]
([*1]*Dept. of Pharmacy*, [*2]*Dept. of Outpatient Chemotherapy Unit*, [*3]*Dept. of Surgery*, [*4]*Dept. of Medical Oncology*, *Hirosaki University Hospital*)

Summary

A portable infusion pump is essential to sustain the 46-hour continuous administration of 5-fluorouracil in the folinic acid, fluorouracil, and oxaliplatin (FOLFOX) and folinic acid, fluorouracil, and irinotecan (FOLFIRI) protocols in colorectal cancer chemotherapy. However, the accuracy of the 5-fluorouracil dose administered via the infusion pump and patient compliance varies because the infusion rate changes depending on the viscosity of the drug, temperature, etc. In addition, the termination of administration based on the patient's judgment may influence these factors.

In the present study, the amount of 5-fluorouracil remaining in the infusion pump and the administration time were investigated.

As a result, the median amount that was found to remain in the pump was 49 mg, which was 2.0% of the average dosage, and an median administration time delay of 70 min was obtained. A questionnaire survey revealed that a majority of the patients felt insecurity about inadequate administration and administration time delays. These results indicate that customizing capacity modulation in the infusion pump corresponding to the patient's usage or seasonal variability of air temperature, and patient education may be important to improve patient compliance. Key words: Cancer chemotherapy, 5-fluorouracil, Portable infusion-pump (*Received Jul. 7, 2009/Accepted Sep. 11, 2009*)

要旨 大腸癌の標準治療であるFOLFOXおよびFOLFIRI療法では，46時間にわたる5-FUの持続投与にインフューザーポンプの使用が必要不可欠である。しかし，その注入速度は薬液の粘度や気温などにより変わる他，患者による自己抜針が行われているため投与精度やコンプライアンスの実態は不明である。そこで，外来治療における5-FU残量と投与時間の実態を調査した。その結果，平均投与量の2%に当たる49 mgの残量および70分の投与時間の遅れを認めた。また，ポンプ使用感に関するアンケートでは，薬剤が適正に投与されているか心配であるとの回答や終了時間が遅れると困るという意見が過半数を占めた。以上より，季節的な気温の影響を考慮し，患者に応じた容量調節や患者指導の徹底などコンプライアンス向上に重要であると思われた。

はじめに

進行再発大腸癌の標準的化学療法であるFOLFOXおよびFOLFIRI療法は投与時間の長さもあり，在宅で5-fluorouracil（以下，5-FU）持続投与を行うケースが多く，その持続投与を目的として携帯バルーン型インフューザーポンプ（以下，ポンプ）が頻用されている。ポンプは，バルーンの収縮力を利用して充填した薬液を持続注入できる医療器具であり，これまで抗癌剤の持続点滴があるため入院を要していたレジメンに対しても，

[*1] 弘前大学医学部附属病院・薬剤部
[*2] 同 ・外来化学療法室
[*3] 同 ・消化器・乳腺・甲状腺外科
[*4] 同 ・腫瘍内科

連絡先: 〒036-8563 弘前市本町53 弘前大学医学部附属病院・薬剤部 腫瘍センター
佐藤 淳也

表1 インフューザーポンプの投与誤差

	全体	ポンプ別内訳	
		バクスター SV2	ニプロ SFS-1002D
投与件数（人数）	646（56）	297（35）	349（33）
投与回数（回）	8.0±6.7	8.9±7.5	9.7±5.9
5-FU 投与量（mg）	2,599±514	2,746±583	2,474±407
生理食塩液量の変更を要した回数（人数）	30（20）	13（8）	17（12）
5-FU 残量（mg）	49±106	42±141	50±54
5-FU 残量/投与量（%）	2.0±3.5	1.7±4.5	2.1±2.1
推定追加投与時間	62±124	94±167	58±70
終了時間誤差（分）	70±157	110±140	15±159

中央値±標準偏差（ただし 5-FU 投与量は平均値±標準偏差）

ポンプの使用により外来・在宅施行が可能となる点で医療経済的有用性も高い[1]。しかし，ポンプの注入速度は薬液の粘度や温度，高低差，静脈圧により変わる他，大腸癌の在宅化学療法の場合，患者自己抜針により投与が終了されているため，ポンプの投与精度や患者の認識と理解度に影響されるコンプライアンスの実態は不明である。

そこで，ポンプでの投与開始から自己抜針までの投与時間とポンプ残重量から求めた 5-FU 残量の実態を調査した。また，投与時間と残量誤差の原因を検討するため，これら誤差と実施月の気温との関連やポンプ使用感に関するアンケート調査を行った。

Ⅰ．方　法

1．対　象

2007 年 7 月～2008 年 12 月までに弘前大学医学部附属病院外来化学療法室にてポンプを使用していた患者 56 名（バクスター SV2 使用患者 35 名，ニプロ SFS-1002D 使用患者 33 名，うち 11 名は両ポンプを使用）を対象に，5-FU 残量と投与時間を調査した。また，同意を得た患者 38 名を対象に，ポンプ使用感についてアンケート調査を行った。以上の調査は，あらかじめ院内の倫理委員会の審査を経た上で実施した。

2．5-FU 残量および投与時間誤差の測定

5-FU 投与時間は，外来化学療法室におけるポンプ接続および在宅における自己抜針時刻から算出した。投与終了後のポンプは，クレンメを閉じた状態で専用の廃棄バッグに入れて次回来院時に持参するよう依頼し，5-FU 残量はその際の回収ポンプ重量を電子天秤（エー・アンド・デイ EW-1500i）にて測定し，空重量との差から算出した。コンプライアンスの指標となる 5-FU 残量および投与時間誤差はいずれも中央値±標準偏差として比較した。ポンプの初期容量は，5-FU 投与量に対してメーカー指定値になるよう生理食塩液で希釈充填したが，回収したポンプのバルーン収縮状態と予定終了時間とのずれを考慮して調節した。すなわち，原則としてバルーンが適切に収縮しているにもかかわらず 3 回連続して±2 時間以上の投与時間誤差を生じた場合，それら平均時間誤差を補正するように生理食塩液量を増減した。また，気温による投与誤差への影響を検討するために，使用した平均気温は気象庁発表の実施月における青森県弘前地区の平均気温を参照した[2]。

3．ポンプ使用感に関するアンケート調査

主な質問項目として，①装着中に薬液が減っているか心配か，②薬液の減少を確認しているか，③終了時間が変わると生活上困るか，④装着中日常生活に影響あるかを設けた。①，③，④については，「とてもそう思う」から「まったくそう思わない」の段階的 5 択の回答を設け，②は頻度について複数の回答を用意した。

Ⅱ．結　果

1．5-FU 残量および投与時間誤差

56 名を対象として調査期間に 646 回の投与が行われ，平均投与量 2,599±514 mg に対する 5-FU 残量の中央値（±標準偏差）は 49（±106）mg（投与量に対して 2.0（±3.5）%）であった。また，投与時間誤差は規定の 46 時間に対して 70（±157）分の遅れを認めた（表 1）。さらに，5-FU 残量と投与時間誤差の分布は，おおむね投与が正確と思われる設定投与量に対する残量 2%以内かつ投与時間誤差±60 分以内に収まるものが 26.6%であった（図 1）。

2．5-FU 残量および投与時間誤差の月別変動

5-FU 残量については，冬期（11～1 月）に低下するものの，他 2～10 月において気温との関連性は見受けられなかった。一方，投与時間誤差は平均気温が比較的高い 8～10 月に少ない傾向にあった（図 2）。5-FU 残量および投与時間誤差に影響する因子として気温および投与量，投与回数，ポンプ種，性別を含めた重回帰分析を行っ

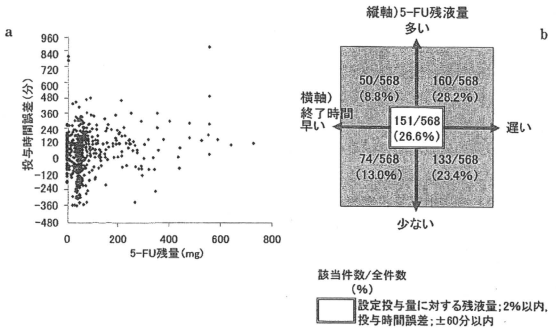

図 1　残液量と投与時間誤差の分布（a: 散布図，b: マトリックス）

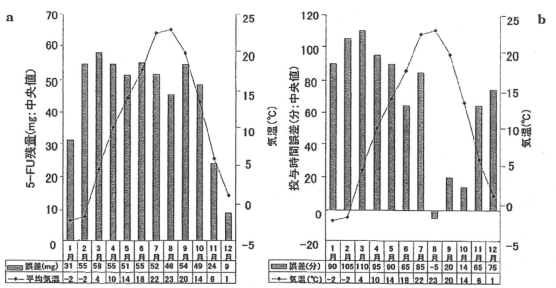

図 2　平均 5-FU 残量（a），投与時間誤差（b）の月別変動

た結果，投与時間誤差と気温の間に統計的有意な負の相関を認めた（$p<0.01$）。

3．使用感に関するアンケート調査

アンケート回答者 38 名のプロフィールは男性 22 名および女性 16 名，平均年齢 63 歳，平均施行回数 11.4 回，使用ポンプについては，ニプロ製のみ 19 名，バクスター製のみ 9 名，両ポンプの使用経験あり 10 名であった。①「装着中に薬液が減っているか心配か」についての回答は，とてもそう思う 29%，ややそう思う 31%，あまりそう思わない 26%，まったくそう思わない 11%，わからない・回答なし 3%であった。②「薬液の減少を確認しているか」については，していない 16%，1 日 1 回 32%，1 日 2〜3 回 34%，1 日 4 回以上 18%であった。③「終了時間が変わると生活上困るか」については，とてもそう思う 16%，ややそう思う 18%，あまりそう思わない 37%，まったくそう思わない 18%，わからない・回答なし 11%であった。④「装着中日常生活に影響あるか」については，とてもそう思う 29%，ややそう思う 24%，あまりそう思わない 41%，まったくそう思わない 3%，回答なし 3%であった。

Ⅲ．考　察

当院では，外来患者への FOLFOX および FOLFIRI 療法はポンプへの薬液充填に加え，分子標的薬を併用した多彩な薬物療法に関する患者指導や副作用対策などの薬学的支援の重要性もあり，外来化学療法室で治療が行われている。患者には専用に作成した教育用 DVD を視聴させ，リーフレットを配布するなどしてポンプ管理から副作用対策の患者指導を行っている。しかし，規定時間に終了しない，あるいは薬液が残っていても早期に自己抜針する例を散見し，バルーンの完全収縮がわかりにくい，ポンプがかさばるなどの患者の意見が寄せられていた。また，入浴ができないなど日常生活上の不都合を訴える患者も多く，規定時間に投与が終了しない場合，QOL 低下は大きいと推測される。そこで，ポンプ接続開始から自己抜針までの投与時間と回収したポンプ内の 5-FU 残量を測定することにより，コンプライアンスの実態を retrospective に調査し，気温などの誤差要因の

把握と使用感の調査を行った。

一般にポンプは薬液粘度や流量制御部の温度，バルーンと末端部の高低差，静脈圧の影響を受け，バクスター製ポンプの場合，規定流速±10%の精度で薬液を持続注入するよう設計されている[3]。実臨床では，薬液粘度が投与量として，温度が投与時期の外気温や室内温度と着衣の状況として，高低差がポンプの装着状況として流速に対する誤差要因となり，投与時間や残量へ影響すると考えられる。さらに調製者の手技の影響も指摘され，実臨床ではこれらの要因が相加的に関連しているものと思われる[4,5]。一連の誤差要因を考慮する上で，特に温度の影響は大きいと推測される。バクスター製ポンプの場合，規定の33.3℃から1℃上昇すると2.3%流速が速まり，逆に1℃低下すると2.3%遅くなるとされているが，今回の調査のように夏期と冬期で平均気温差が20℃以上ある状況で，投与誤差の季節変動をみた報告はない。同じポンプを使用した林らの報告によれば，たとえ流量制御部の温度が33℃であっても，本体の温度がそれぞれ22℃および4℃に低下した場合，5～7%および26～28%低下するとしている。また，流速や流出時間に影響する因子として体部に密着し，温度変化の影響を緩衝する流量制御部があっても本体温度が流速に大きな影響を与えると指摘している[6]。

今回，冬期の終了時間が夏期に比べ遅れた結果は，冬期はポンプ本体の温度低下が流速の低下を生じ，バルーンの完全収縮まで自己抜針を待ったため投与時間の遅延が大きくなったと推測される。さらに患者によっては就寝時，体幹付近にポンプを置かず枕元にポンプをだす患者もおり，室内であっても気温の低下する冬期の遅延が大きかったと思われる。

今回の調査背景には，ポンプ充填量をメーカー指定値に合わせ治療を開始したが，使用回数に応じて一定以上の投与時間誤差を生じた場合，充填する生理食塩液量を調節する補正を加えている。臨床では，患者の理解度があり適正使用されている状況で，計量誤差を超える誤差が偶発的でなく3回以上という再現性をもって発生する場合，希釈量を調節せざる得ない状況にある。これら補正を加えても，5-FU残量が投与量の2%以内（2,500 mgでは50 mg以内），投与時間誤差が60分以内というおおむね正確な使用状況は投与件数の26.6%にすぎず，5-FU残量が多いにもかかわらず抜針時間が早すぎる，あるいは5-FU残量が少ないにもかかわらず抜針時間が遅すぎる（図1bの左上および右下のマトリックス）場合が32.2%，規定終了時間を越えても5-FU残量が多い，あるいは抜針時間が早いにもかかわらず5-FU残量がない（右上および左下のマトリックス）場合が41.2%存在した。前者はさらに適正使用に向けて患者指導を要する場合であり，後者は医療者側が生理食塩液量の調節を要する場合であり，コンプライアンス向上を目的とした患者指導や充填量の調節がこれらの頻度で必要であると思われた。

アンケート調査では，「薬液が減っているか心配か」との質問には，60%がそう思うと回答したものの，そう思わないという回答も37%あった。また，「薬液の減少を確認しているか」については，1日1回以上している回答が84%あるが，まったくしていないという回答も16%あった。さらに，「ポンプの装着は日常生活に影響あるか」については，53%がそう思うと回答していたのに対して，そう思わない，あるいはわからないなど否定的な回答が44%を占めた。薬液の減少に不安を感じバルーン収縮を比較的頻回に確認している患者群は，仕事や社会活動が現役の患者に多く，一方これが気にならずあまり確認していない患者群は，抜針時間が遅れても社会活動に影響のない高齢者に多いことが回答を二極化させた理由であると思われる。また，日常生活へのポンプ装着の影響は，予想に反し影響あるとの回答が少なかったが，当院では充填量が100 mL以下のコンパクトなポンプを使用していたことが日常生活への影響が最小化された要因であると思われた。容量の異なる複数のポンプを使用している患者に対するQOL調査を行った亀井らの報告でも，小容量のポンプ使用が日常生活への制限を少なくするという結果が得られている[7]。

以上より，ポンプによる5-FU投与誤差は想像以上に大きく，使用中の日常生活に不便を感じている患者群も存在した。bevacizumabの登場によりFOLFOXおよびFOLFIRI療法の奏効期間が長くなるなかで，形状がコンパクトで残量のわかりやすいポンプの使用や季節性を考慮したモニタリングと患者ごとの充填量の調節，患者指導が重要であると思われた。

文　献

1) 田中真伸，櫻田　睦，鎌野俊紀・他：持続注入ポンプを用いた外来在宅大腸癌化学療法と経済効果．外科治療　89(5)：603-604，2003.
2) 気象庁，気象統計情報，http://www.data.jma.go.jp/obd/stats/etrn/index.php
3) バクスターインフューザー（SVシリーズ（ボトルタイプ）・LVシリーズ）製品添付文書（2008年2月1日改訂第8版）．
4) 木村　緑，小林政彦，乾　賢一・他：外来化学療法における携帯型持続注入器の精度調査．日病薬師会誌　44(10)：1507-1510，2008.
5) 丸山昌広，荒川裕貴，恩田久美子・他：バルーンインフューザーポンプの大腸がん化学療法（FOLFOX4療法）における流出速度について．日病薬師会誌　44(6)：905-908，2008.
6) 林　秀樹，神戸宏憲，伊藤邦彦・他：がん化学療法における携帯型ディスポーザブル注入ポンプの流速変動因子の

解析．日病薬師会誌　45(6):821-824, 2009.
7) 亀田彩子，熊谷範之，松浦　誠・他:携帯型持続注入器を用いた5-FU持続投与法が日常生活に与える影響．医薬品相互作用研究　32(2):69-73, 2008.

Lung Cancer 68 (2010) 204–210

Contents lists available at ScienceDirect

Lung Cancer

journal homepage: www.elsevier.com/locate/lungcan

Clinical characteristics of pleomorphic carcinoma of the lung

Kenichiro Ito[a], Satoshi Oizumi[a,*], Shinichi Fukumoto[b], Masao Harada[b], Takashi Ishida[c], Yuka Fujita[d], Toshiyuki Harada[e], Tetsuya Kojima[f], Hiroshi Yokouchi[g], Masaharu Nishimura[a], Hokkaido Lung Cancer Clinical Study Group

[a] First Department of Medicine, Hokkaido University School of Medicine, North 15, West 7, Kita-ku, Sapporo 060-8638, Japan
[b] Department of Pulmonary Diseases, National Hospital Organization Hokkaido Cancer Center, Sapporo, Japan
[c] Department of Pulmonary Medicine, Fukushima Medical University School of Medicine, Fukushima, Japan
[d] Department of Respiratory Medicine, National Hospital Organization Dohoku National Hospital, Asahikawa, Japan
[e] Section of Respiratory Diseases, Department of Internal Medicine, Hokkaido Social Insurance Hospital, Sapporo, Japan
[f] Department of Medical Oncology, KKR Sapporo Medical Center, Sapporo, Japan
[g] Department of Medicine, Hokkaido Chuo Rosai Hospital, Iwamizawa, Japan

ARTICLE INFO

Article history:
Received 16 December 2008
Received in revised form 3 May 2009
Accepted 2 June 2009

Keywords:
Pleomorphic carcinoma
FDG-PET
Surgery
Chemotherapy
Gefitinib
Prognosis

ABSTRACT

Background: Pleomorphic carcinoma of the lung is a malignant epithelial tumor that contains carcinomatous and sarcomatoid components. Due to its rarity, few studies have been reported, and its clinical and pathological characteristics remain unclear.
Method: We retrospectively investigated 22 cases of pleomorphic carcinoma of the lung.
Results: Fifteen cases were diagnosed by surgical resection, 4 by autopsy, and 3 by transbronchial biopsy. Nineteen patients were male and 3 were female, and their mean age at diagnosis was 68.3 years (±10.1). Eighteen were current- or ex-smokers with substantial smoking histories (mean 46.4 pack-years). Sixteen patients had symptoms: hemoptysis and cough were commonly seen. Chest computed tomography (CT) findings revealed that the tumors were quite large (mean diameter 45.3 ± 21.9 mm; range 14–110 mm), and 21 tumors were peripherally located. Positron emission tomography with 18-fluorodeoxy-glucose (FDG-PET) was performed in 12 patients, and the Standardized Uptake Value (SUV) tended to be high (9.44 ± 4.98). In the 15 patients who underwent surgical resection, recurrence was common; systemic metastases were also frequently found. Patients who had received surgical treatment with proper follow-up care survived longer than those who did not undergo surgery. Responses to chemotherapy were generally poor, although 1 patient exhibited partial response to gefitinib.
Conclusions: Pulmonary pleomorphic carcinoma has strong malignant potential with frequent distant metastases, as has already been reported. However, this study demonstrated that surgical treatment and appropriate follow-up therapy might result in better prognoses.

1. Introduction

According to the World Health Organization classification of lung tumors, pleomorphic carcinoma of the lung is one of five subgroups of sarcomatoid carcinoma [1], which itself is defined as a group of poorly differentiated tumors characterized pathologically by a combination of epithelial and mesenchymal elements. Pleomorphic carcinoma is histologically defined as either non-small cell carcinoma combined with neoplastic spindle and/or giant cell or a carcinoma that consists of only spindle cell and giant cell. At least 10% of the neoplasm should be pleomorphic.

If the tumor consists of only spindle cells or only giant cells, it is defined as a spindle cell or giant cell carcinoma, respectively, which are other subgroups of sarcomatoid carcinoma. Carcinosarcoma, which contains carcinoma and sarcoma, is another subgroup. Sarcoma components differentiate to osteosarcoma, chondrosarcoma, and rhabdomyosarcoma. Bone, cartilage, muscle, fat, and neuron are sometimes detected pathologically in tumors. Pulmonary blastoma is a very rare type of sarcomatoid carcinoma characterized as biphasic tumor containing a primitive epithelial component resembling well-differentiated fetal-type adenocarcinoma and a primary mesenchymal stroma.

Since its diagnostic criteria were confirmed, pulmonary pleomorphic carcinoma has been diagnosed more frequently. It is essential to understand its clinical behavior for effective management of patients with this disease. However, as pulmonary pleomorphic carcinoma is rare (only 0.1–0.4% of all malignant

* Corresponding author. Tel.: +81 11 706 5911; fax: +81 11 706 7899.
E-mail address: soizumi@med.hokudai.ac.jp (S. Oizumi).

0169-5002/$ – see front matter © 2009 Elsevier Ireland Ltd. All rights reserved.
doi:10.1016/j.lungcan.2009.06.002

tumors of the lung) [2–4], its clinical and pathological characteristics are not well known. We have retrospectively investigated 22 patients with pulmonary pleomorphic carcinoma diagnosed by surgical resection, autopsy, or transbronchial biopsy (TBB). Radiological findings, results of positron emission tomography with 18-fluorodeoxy-glucose (FDG-PET), treatment, and clinical course are described in this report.

2. Material and methods

2.1. Patients

We retrospectively analyzed 22 pulmonary pleomorphic carcinomas from a total of 2447 primary lung cancers (including 1022 cases of resected lung cancer) that we experienced between January 2005 and December 2008 at seven institutes (Hokkaido University Hospital, National Hospital Organization Hokkaido Cancer Center, Fukushima Medical University School of Medicine, National Hospital Organization Dohoku National Hospital, Hokkaido Social Insurance Hospital, Hokkaido Chuo Rosai Hospital, and KKR Sapporo Medical Center). Pathological diagnosis was made by surgical resection, autopsy, or TBB. The incidence of pulmonary pleomorphic carcinoma was 0.90%. This study was approved by the institutional review boards of each institute, and all patients provided written informed consent.

2.2. CT and FDG-PET protocol

Chest computed tomography (CT) was performed in all patients. The size, location, and internal density of the tumor, and the presence of a cavity were evaluated. Hilar and mediastinal lymph nodes were measured, and if the short-axis diameter of a lymph node was equal to or longer than 10 mm, it was considered positive. Abdomen CT was also performed to detect metastases to abdominal organs such as liver, kidney, and adrenal gland.

Positron emission tomography with 18-fluorodeoxy-glucose (FDG-PET) has been used for evaluating tumors of the lung as well as lymph node and distant metastases. The Standardized Uptake Value (SUV), which was obtained by placing a region of interest over the lesion and dividing the value (in microcuries per cubic centimeter) by the injected dose (in microcuries) divided by the patient's body weight (in grams) [5], was measured. In this series, 12 patients underwent FDG-PET.

2.3. Pathological diagnosis

Pleomorphic carcinoma was defined as non-small cell carcinoma containing at least 10% sarcomatoid components. Pathologists evaluated specimens that were obtained by surgery, autopsy and TBB. In this study, when a TBB specimen contained both carcinomatous and sarcomatoid components, and the non-small cell lung cancer component was clearly distinct from the spindle/giant cell carcinoma, the tumor was diagnosed as pleomorphic carcinoma.

2.4. Evaluation of response to chemotherapy or radiotherapy

Response evaluations for chemotherapy and/or radiotherapy were assessed using RECIST (Response Evaluation Criteria in Solid Tumors) guidelines [6]. Overall survival was defined as the time from the first day of treatment until death from any cause.

2.5. Statistical analysis

In this paper, statistical values are given as mean ± standard deviation. Continuous variables were compared using the Student's *t*-test or Mann–Whitney test, as appropriate. All survival curves for time-to-event variables were created using the Kaplan-Meier method [7].

3. Results

3.1. Patient characteristics

Patient characteristics are summarized in Table 1. The male:female ratio was 19:3. The age at diagnosis was 68.3 ± 10.1 years (range 51–94). Symptoms were seen in 16 patients (72.7%): common symptoms were hemoptysis (7 cases) and cough (6 cases). Fever, pain, dyspnea and body weight loss were also seen. Six patients (27.3%) had no symptoms but were referred to hospital with lung nodules detected on chest X-rays. Eighteen patients (81.8%) were current- or ex-smokers, and the remaining 4 (18.2%) had never smoked. The smoking history was striking: the mean number of pack-years of the 22 patients was 46.4 ± 36.3, with a maximum value of 160 pack-years (patient 5); the mean value of the 18 smokers was 56.7 ± 31.8 pack-years.

Biochemical examination revealed that in 14 of the 22 cases (63.6%), serum carcinoembryonic antigen (CEA) was high, at 18.1 ± 41.2 ng/ml (normal 1.0–6.5). In 10 of the 18 cases examined (55.6%), cytokeratin fragment 19 (CYFRA 21-1) was also increased (4.0 ± 4.3 mg/ml; range 0.0–14.1; normal 0.0–2.0). No other tumor markers examined, including carbohydrate antigen 19-9 (CA19-9), Sialyl Lewis (x) (SLX), squamous cell carcinoma antigen (SCC-Ag), pro-gastrin-releasing peptide (Pro-GRP), and neuron-specific enolase (NSE), were specific and useful for diagnosis of pleomorphic carcinoma of the lung.

3.2. Radiological findings

Chest CT was performed in all 22 cases and revealed fairly large tumors: 45.3 ± 21.9 mm in diameter (range 14–110). All tumors were observed as mass or nodule, and ground glass opacity pattern or consolidations were not seen in our study. One case (patient 17) had a cavity inside the tumor (tumor diameter 50 mm). Twenty-one tumors (95.5%) were located in the peripheral field of the lung, while 1 was central (patient 20, non-small cell carcinoma + spindle cell). In 15 cases (68.2%), the primary tumor was located in the upper lobe (right: 12 cases; left: 3 cases), and the remaining 7 tumors (31.8%) were located in the middle or lower lobe. Four cases exhibited internal low densities and heterogeneous pattern (patients 1, 14, 15, and 19). At the time of diagnosis, chest wall invasions were found in 2 patients (patients 6 and 17) and clinical T4 disease (malignant pleural and/or pericardial effusion, pleural dissemination, mediastinal invasion, and metastases to the same lobe) in 4 patients (patients 14, 16, 19, and 22). Clinical nodal involvements on CT findings were observed in 13 of the 22 patients (7 of 15 patients who underwent surgical resection).

Twelve patients underwent FDG-PET, and the SUV of the primary lesions tended to be high (9.44 ± 4.98; range 3.00–16.6). SUVs of T1 (≤3 cm) and T2 (>3 cm) disease were 7.16 ± 4.59 and 9.89 ± 5.16, respectively. Most of the metastatic lymph nodes and distant metastases also exhibited high SUV.

3.3. Diagnosis and pathological findings

Fifteen cases of pulmonary pleomorphic carcinoma were diagnosed by surgical resection (Table 1; patients 1–15). Representative histological finding of the resected tumor is shown in Fig. 1A (patient 4, squamous cell carcinoma with spindle cell). Eleven of the 15 tumors were diagnosed as primary lung cancer by sputum and/or transbronchial brushing cytology, or TBB before surgery. Another 4 cases (Table 1; patients 16–19) were confirmed by autopsy to have

Table 1
Clinical and pathological findings of 22 patients with pleomorphic carcinoma of the lung.

Patient no.	Sex	Age (years)	Smoking history (pack-years)	Symptoms	CEA (ng/ml)	Pathological subtypes		c-Stage	p-Stage
						Carcinomatous component	Sarcomatoid component		
Surgical resection									
1	M	79	75	Hemoptysis, body weight loss	7.7	Large cell carcinoma	Giant cell	cT2N1M0 IIB	pT3N2M0 IIIA
2	M	67	42	None	12.4	Adenocarcinoma	Giant cell	cT1N0M0 IA	pT1N0M0 IA
3	M	70	37.5	Fever	8.8	Large cell carcinoma	Giant cell	cT2N1M0 IIB	pT2N0M0 IB
4	M	77	35.6	Hemoptysis	8.1	Squamous cell carcinoma	Spindle cell	cT2N2M0 IIIA	pT4N2M0 IIIB
5	M	77	160	None	9.8	Large cell carcinoma	Spindle cell	cT2N1M0 IIB	pT2N1M0 IIB
6	M	59	51.3	None	6.6	Adenosquamous cell carcinoma	Spindle cell	cT3N0M0 IIB	pT3N0M0 IIB
7	M	64	66	Hemoptysis, cough	2.3	Adenocarcinoma	Spindle cell	cT2N0M0 IB	pT3N0M0 IIB
8	M	64	67.5	Hemoptysis	7.5	Adenocarcinoma	Spindle cell	cT2N0M0 IB	pT2N0M0 IB
9	F	70	0	Cough	12.8	Adenocarcinoma	Spindle cell	cT1N0M0 IA	pT1N0M0 IA
10	M	73	31.8	Hemoptysis	8.3	Squamous cell carcinoma	Spindle cell + Giant cell	cT2N2M0 IIIA	pT2N2M0 IIIA
11	M	71	56	Dyspnea	3.4	Adenocarcinoma	Giant cell	cT2N2M0 IIIA	pT2N1M0 IIB
12	M	74	50	Hemoptysis	2.8	Large cell carcinoma	Giant cell	cT2N0M0 IB	pT2N0M0 IB
13	M	68	55	None	1.3	Large cell carcinoma	Giant cell	cT1N0M0 IA	pT1N0M0 IA
14	M	51	33.8	Dyspnea, cough	0.7	Non-small cell carcinoma	Giant cell	cT4N0M0 IIIB	pT4N0M0 IIIB
15	M	54	82.5	None	2.7	Adenocarcinoma	Giant cell	cT2N2M1 IV	pT4N0M1 IV
Autopsy									
16	M	73	75	Dyspnea, back pain	197	Large cell carcinoma	Spindle cell + Giant cell	cT4N3M1 IV	
17	M	52	30	Hemoptysis, cough	37.2	Squamous cell carcinoma	Spindle cell + Giant cell	cT3N2M1 IV	
18	M	57	60	Cough, sputum fever	15.4	Large cell carcinoma	Giant cell	cT2N3M0 IIIB	
19	F	63	0	Cough, fever	4.4	Adenocarcinoma	Giant cell	cT4N1M1 IV	
TBB (transbronchial biopsy)									
20	M	94	0	None	8.1	Non-small cell carcinoma	Spindle cell	cT1N0M0 IA	
21	F	70	0	None	38.4	Large cell carcinoma	Giant cell	cT2N3M1 IV	
22	M	76	12.5	Back pain	2.9	Adenocarcinoma	Spindle cell	cT4N2M0 IIIB	

CEA: carcinoembryonic antigen.

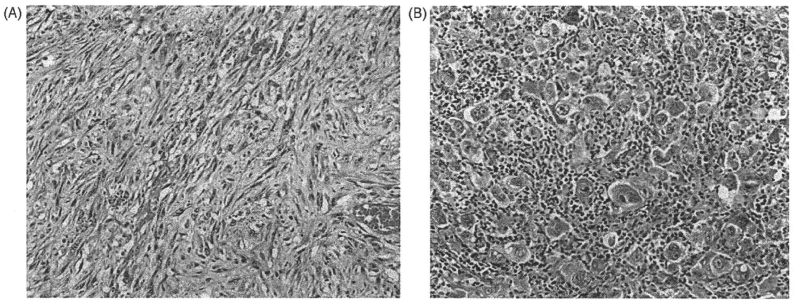

Fig. 1. Histological findings of pleomorphic carcinoma. (A) A spindle cell carcinoma component seen in a surgically resected tumor (patient 4, hematoxylin and eosin, 100×). (B) A giant cell carcinoma component in a tumor tissue obtained by transbronchial biopsy (patient 21, hematoxylin and eosin, 100×).

pulmonary pleomorphic carcinoma. In the other 3 patients (Table 1; patients 20–22), sarcomatoid elements were successfully detected with TBB (Fig. 1B, patient 21, large cell carcinoma with giant cell), and pleomorphic carcinoma was diagnosed without surgical resection or autopsy.

Sputum cytology was performed in 15 patients. In 2 patients (13.3%), carcinoma cells but not sarcomatoid elements were detected: 1 case (patient 10) was diagnosed as squamous cell carcinoma and the other (patient 4) as adenosquamous cell carcinoma.

Transbronchial brushing cytology and/or TBB was performed in 21 patients, confirming 17 cases of lung cancer. In 7 of the 17 cases, sarcomatoid elements were pathologically obtained in specimens. Three (patients 1, 9, and 11) of these patients received surgical resection, and 1 (patient 18) underwent autopsy. The other 3 (patients 20–22) patients were diagnosed with pleomorphic carcinoma by the TBB results alone without surgery or autopsy.

We also investigated differences in clinical features according to pathological subtypes. Large cell carcinoma combined with giant cell (6 cases, 27.3%) and adenocarcinoma combined with spindle cell (4 cases, 18.2%) were predominantly observed. We did not find any statistical differences in clinical or radiological characteristics according to pathological subtypes.

3.4. Clinical course and prognosis for patients having surgical treatment

Clinical stages at the point of diagnosis were stage IA in 4 cases (18.2%), stage IB in 3 cases (13.6%), stage IIB in 4 cases (18.2%), stage IIIA in 3 cases (13.6%), stage IIIB in 3 cases (13.6%), and stage IV in 5 cases (22.7%) (Table 1). Of the 15 patients with surgical resection (patients 1–15), pathological stage (p-stage) was upgraded compared with clinical stage (c-stage) in 4 cases (26.7%). Pathological stages were stage IA in 3 cases (20%), stage IB in 3 cases (20%), stage IIB in 4 cases (26.7%), stage IIIA in 2 cases (13.3%), stage IIIB in 2 cases (13.3%), and stage IV in 1 case (6.7%) (Table 1). Fig. 2A shows overall Kaplan-Meier survival curve in all of the enrolled 22 patients. Median survival time (MST) was 213 days.

Of the 15 patients who underwent surgery, 6 patients, including 5 with pN0 disease, relapsed after surgery. Four of them had recurrence by distant metastases (2 to the brain, 1 to lung, and 1 to bone). Four of these patients died from relapsed cancer, while 2 patients (patients 9 and 15) are still alive (1 of them is receiving gefitinib). The other 9 patients have not developed any recurrence at the time of analysis, including 2 patients who died of non-cancer-related disease (pneumonia and heart disease).

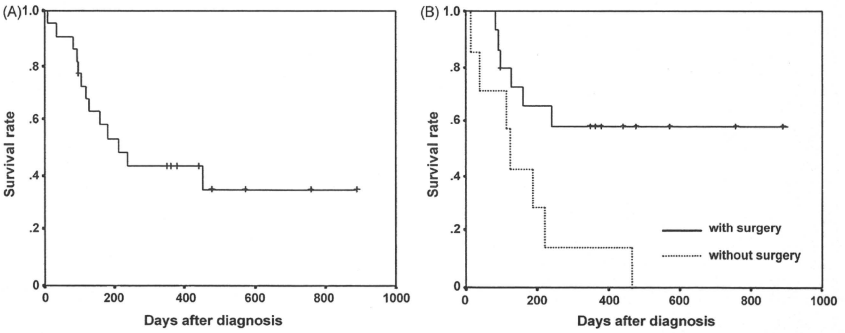

Fig. 2. (A) Kaplan-Meier overall survival of all patients and (B) overall survival of patients treated with surgery (15 patients) or without surgery (7 patients).

Table 2
Summary of chemotherapy for 5 patients except for adjuvant therapy.

Patient no.	Situation	Stage	Regimens (best response)
9	Recurrence after surgery	pT1N0M0 IA	CDDP/DOC (SD) → Gef (PR)
15	Recurrence after surgery	pT4N0M1 IV	CBDCA/PTX (SD)
17	No indication of surgery	cT3N2M1 IV	CBDCA/PTX (SD) → GEM/VNR (PD) → Gef (NE[a]) → S-1 (PD)
18	No indication of surgery	cT2N3M0 IIIB	CBDCA/PTX (SD) → GEM/VNR (NE[a])
19	No indication of surgery	cT4N1M1 IV	CBDCA/DOC (SD)

CDDP: cisplatin, DOC: docetaxel, Gef: gefitinib, CBDCA: carboplatin, PTX: paclitaxel, GEM: gemcitabine, VNR: vinorelbine, S-1: TS-1, PR: partial response, SD: stable disease, PD: progressive disease, NE: not evaluated.
[a] Occurred drug-induced interstitial pneumonitis.

Four patients (patients 1, 6, 10, and 14) received adjuvant chemotherapy post-surgery. Patient 6 exhibited pT3N0M0 (stage IIB) with chest wall invasion and received chemo-radiation therapy (cisplatin plus docetaxel and 65 Gy radiation in total). This patient was still alive without recurrence 441 days after surgery. Other 3 patients received chemotherapy alone. Patient 1 received UFT (Tegafur/Uracil) and was alive without recurrence 573 days after surgery. Patient 10 had adjuvant chemotherapy with vindesine, UFT, and OK432. This patient had recurrence 78 days after surgery and died after 126 days. Patient 14 received carboplatin and gemcitabine and was alive 98 days after surgery.

Patients 9 and 15 received chemotherapy for a recurrent tumor after surgery (Table 2). Patient 9 received cisplatin plus docetaxel as first-line therapy, and the response was stable disease (SD). It is noteworthy that the case (a 70-year-old non-smoker woman) exhibited partial response to gefitinib as second-line therapy. The pathological subtype of this case was adenocarcinoma combined with spindle cell. Interestingly, the tumor harbored epidermal growth factor receptor (EGFR) mutations (L858R).

Fig. 2B shows overall Kaplan-Meier survival curve in the 15 patients who underwent surgical resection. Nine patients were still alive at the time of analysis, and MST was not determined.

3.5. Clinical course and prognosis for patients who did not undergo surgery but received chemotherapy, radiotherapy, or best supportive care

Four (patients 16, 17, 19, and 21) of the 7 cases who did not undergo surgical resection (patients 16–22) and one (patient 15) of patients who received surgery had distant metastases at the time of diagnosis (stage IV). The metastasis sites were bone (2 cases), lung, adrenal gland, skin, and lymph node (1 case each). Three patients (patients 18, 20, and 22) did not have surgical treatment because they had c-stage IIIB disease (patients 18 and 22) or advanced age (patient 20; 94 years old). During their clinical course, other metastases to brain, liver and the small intestine appeared. One patient (patient 18) died of perforation of the small intestine because of metastasis. Autopsy (patients 16–19) revealed small metastases to heart, kidney, thyroid gland and distant lymph nodes that could not be proven by CT or MRI before death. Fig. 2B shows Kaplan-Meier overall survival curve for the 7 patients who did not undergo surgery; MST was 118 days.

Three patients received chemotherapy against advanced tumor without surgical resection (patients 17, 18, and 19). As first-line therapy, the patients received carboplatin plus paclitaxel (patients 17 and 18) and carboplatin plus docetaxel (patient 19). Two received gemcitabine plus vinorelbine as second-line treatment (patients 17 and 18). Only patient 17 received gefitinib as third-line and TS-1 as fourth-line treatments. Response was very poor, as shown in Table 2 (there were two NE (not evaluated) cases because of difficulties in performing follow-up examinations after onset of acute drug-induced pneumonitis). Even with first-line chemotherapy, no partial response was observed with the cytotoxic agents. The MST of these 3 patients (who did not undergo surgical treatment) was 213 days.

A total of 6 patients received irradiation for primary tumor causing back pain (patient 22), for brain metastasis (patient 8), for bone metastasis (patients 9 and 21), and as adjuvant therapy after surgical resection for pT3 tumors (patients 6 and 7).

Two of 22 patients received best supportive care because of advanced age and poor Eastern Cooperative Oncology Group Performance Status (ECOG PS) (patients 16 and 20).

4. Discussion

Lung tumors have been reclassified by the World Health Organization. In 1999, a group named "carcinoma with pleomorphic, sarcomatoid, or sarcomatous elements" was defined. In 2004, this group, which contained pleomorphic carcinoma, was renamed "sarcomatoid carcinoma" [1]. Travis et al. had previously reported pleomorphic carcinoma of the lung to be very rare (approximately 0.1–0.4% of all lung malignancies) [2–4]. Since its pathological definition became widely recognized, pleomorphic carcinoma has been diagnosed more frequently: in our study, its frequency was 0.90% (22/2447 cases). In another recent study, it was found to be 1.6% (45/2743) of resected non-small cell lung cancer (NSCLC) [8]. As in previous reports [8–12], most cases in our study were male with a history of smoking; they exhibited symptoms such as hemoptysis and cough.

Pleomorphic carcinoma of the lung was often found as a large mass, more than 4–5 cm in diameter. In our study, the tumors tended to be located in the periphery of the upper lobes. Frequently observed hemoptysis might be characteristic of pulmonary pleomorphic carcinoma in spite of its peripheral location. We discovered sarcomatoid elements in 7 cases by transbronchial brushing cytology and/or biopsy; however, there were no cases diagnosed only with cytological examination. Even when the component is included in the specimen, definite diagnosis of pleomorphic carcinoma should be avoided because it is difficult to differentiate the spindle component from active fibroblasts, as well as a giant cell component from multinucleated histiocytes. Kim et al. reported that 86% of pulmonary pleomorphic carcinomas with an adenocarcinoma component and 100% of those with a large cell carcinoma component were located in the periphery, while 100% of the pleomorphic carcinomas with a squamous cell carcinoma component were located in the central region [10].

They also demonstrated that the CT features of the tumor appeared to be dictated by its epithelial components. However, in our study, only 1 tumor was centrally located, the subtype of which was non-small cell carcinoma combined with spindle cell. All 3 cases of pulmonary pleomorphic carcinomas with a squamous cell carcinoma component were located in the periphery. In addition, CT features such as a cavity and heterogeneous density in the tumor that reflected necrosis or hemorrhage were not related to tumor subtypes. Neither patient characteristics (age, sex, smoking history, and symptoms), FDG-PET findings, response to chemotherapy, nor prognosis differed significantly between pathological subtypes. Mochizuki et al. also described that there were no significant differences in the overall survival between groups divided by predominant epithelial component [12].

FDG-PET was useful in examining patients with pleomorphic carcinoma of the lung, because it showed higher SUV in primary lesions even if the size of the tumor was small (minimum size was 15 mm in the 12 examined cases). SUVs of T1 (≤3 cm) and T2-4 (>3 cm) disease were 7.16 ± 4.59 and 9.89 ± 5.16, respectively. Tournoy et al. has reported mean SUVs of T1 and T2-4 NSCLC as 3.71 and 5.20 [13]. There was a statistically significant difference in SUV of T2-4 diseases between NSCLC and pleomorphic carcinoma ($P < 0.01$), whereas there was no significant difference in SUV of T1 diseases ($P = 0.48$). Although there were only 2 T1 tumors in our study, our FDG-PET result suggests that the SUV of pleomorphic carcinoma might be higher than that of common non-small cell lung cancer, which might be helpful in diagnosis.

Biochemical examination revealed serum CEA to be elevated in 63.6% of patients (14 cases). This marker is known to be specific for other tumors including adenocarcinoma and is affected by external factors such as smoking. SCC, CYFRA, SLX, Pro-GRP, and NSE were considered to be non-specific markers for pulmonary pleomorphic carcinoma.

Distant metastasis was frequently observed in patients with pleomorphic carcinoma of the lung. The major sites of distant metastases were the same as those for other malignant epithelial lung tumors, i.e., bone, brain, lung, liver and adrenal gland, but the progression of this tumor is particularly rapid, and distant metastases seem to strongly influence prognosis. Autopsies revealed that pleomorphic carcinomas of the lung tended to expand into various lesions: minor sites of metastases such as thyroid grand, peritoneum and lymph nodes of abdomen could not be found by clinical examination before death. In particular, metastases to small intestine were revealed by autopsy in 2 patients, 1 of whose death (patient 18) was a result of intestine perforation.

Chest wall invasions and mediastinal invasions were commonly observed in the 15 patients who underwent surgical resection, as postoperative pathological findings rather than preoperative prediction. Because of pT3 disease, 3 cases were given adjuvant therapy (irradiation (patient 7) or chemotherapy (patient 1) or chemo-radiation therapy (patient 6)). Recurrence after surgery was frequently observed, and it should be noted that 5 cases with pN0 disease also relapsed. While Raveglia et al. reported that nodal involvement was a determinant prognostic variable of pleomorphic carcinoma of the lung [9], Yuki et al. commented that even patients with pN0 disease frequently experienced vascular invasion (57.1%) [8]. We have to keep in mind that pleomorphic carcinoma of the lung has the potential to recur even if the primary lesion is resected at an early stage. In our study, the 15 patients who underwent surgery better prognoses, with 9 patients surviving, compared with a MST of 118 days for patients who had not received surgery. One reason might be that some patients properly received chemotherapy, irradiation, or combination as adjuvant therapy post-surgery or when the relapsed tumor was found; indeed 4 patients receiving the treatments are still alive.

Chemotherapy was administered to 9 patients, 4 of whom received adjuvant chemotherapy after surgery, while the other 5 had recurrence after surgery or advanced cases without surgery; however, neither platinum-based nor non-platinum-based chemotherapy was effective. Bae et al. also commented that advanced pulmonary pleomorphic carcinoma showed poor response to chemotherapy regimens [11]. Of note is the fact that we experienced one partial response to gefitinib despite this being second-line treatment (patient 9). The tumor in this case was diagnosed as pleomorphic carcinoma by surgical resection, and EGFR mutation (L858R) was detected. The presence of EGFR mutation is related to a patient's background and pathological subtypes of the lung cancer: it influences response to gefitinib [14]. This Japanese patient was female with no history of smoking, and the subtype of the tumor was adenocarcinoma combined with spindle cell. She had relapsed 19 months after surgery. First, she received platinum-based chemotherapy, which caused a SD response, and then gefitinib as second-line treatment resulted in survival for 890 days after surgery. It was not clear whether gefitinib was effective for only the adenocarcinoma component and not the spindle cell component since we could not obtain a tumor tissue sample after treatment. However, the good response to second-line gefitinib highlighted the importance of molecular targeted therapy for this entity.

5. Conclusion

In conclusion, we retrospectively analyzed 22 cases of pulmonary pleomorphic carcinoma in a total of 2447 cases of primary lung cancer. Pulmonary pleomorphic carcinoma had strong malignant potential with frequent distant metastases. We demonstrated that surgical treatment and appropriate follow-up therapy including the use of a molecular targeting drug (e.g., gefitinib for patients with adenocarcinoma as carcinomatous component) might improve outcomes. Some other important findings regarding the characteristics and clinical course of the tumor have been described in this report, and further investigations will be needed to elucidate more definitive clinical features and to establish appropriate methodological strategies for pleomorphic carcinoma of the lung.

Conflict of interest

The authors have no conflict of interest to declare.

Acknowledgements

We are grateful to Dr. Koichi Yamazaki, former associate professor of the First Department of Medicine, Hokkaido University School of Medicine, for his outstanding support. We also thank Dr. Yoshihiro Matsuno (Hokkaido University Hospital), Dr. Katsushige Yamashiro (Hokkaido Cancer Center), Dr. Kazuo Watanabe (Fukushima Medical University Hospital), Dr. Yuichiro Fukasawa (KKR Sapporo Medical Center), and Dr. Kenzo Okamoto (Hokkaido Chuo Rosai Hospital), for valuable assistance in pathological diagnosis and review.

References

[1] Beasley MB, Brambilla E, Travis WD. The 2004 World Health Organization classification of lung tumors. Semin Roentgenol 2005;40:90–7.
[2] Brambilla E, Travis WD, Colby TV, Corrin B, Shimosato Y. The new World Health Organization classification of lung tumours. Eur Respir J 2001;18:1059–68.
[3] Travis WD, Travis LB, Devesa SS. Lung cancer. Cancer 1995;75:191–202.
[4] Travis WD. Pathology of lung cancer. Clin Chest Med 2002;23:65–81.
[5] Rohren EM, Turkington TG, Coleman RE. Clinical applications of PET in oncology. Radiology 2004;231:305–32.
[6] Therasse P, Arbuck SG, Eisenhauer EA, Wanders J, Kaplan RS, Rubinstein L, et al. New guidelines to evaluate the response to treatment in solid tumors. J Natl Cancer Inst 2000;92:205–16.
[7] Kaplan EL, Meier P. Nonparametric estimation from incomplete observations. J Am Stat Assoc 1958;53:457–81.
[8] Yuki T, Sakuma T, Ohbayashi C, Yoshimura M, Tsubota N, Okita Y, et al. Pleomorphic carcinoma of the lung: a surgical outcome. J Thorac Cardiovasc Surg 2007;134:399–404.
[9] Raveglia F, Mezzetti M, Panigalli T, Furia S, Giuliani L, Conforti S, et al. Personal experience in surgical management of pulmonary pleomorphic carcinoma. Ann Thorac Surg 2004;78:1742–7.
[10] Kim TS, Han J, Lee KS, Jeong YJ, Kwak SH, Byun HS, et al. CT findings of surgically resected pleomorphic carcinoma of the lung in 30 patients. Am J Roentgenol 2005;185:120–5.
[11] Bae HM, Min HS, Lee SH, Kim DW, Chung DH, Lee JS, et al. Palliative chemotherapy for pulmonary pleomorphic carcinoma. Lung Cancer 2007;58:112–5.
[12] Mochizuki T, Ishii G, Nagai K, Yoshida J, Nishimura M, Mizuno T, et al. Pleomorphic carcinoma of the lung: clinicopathologic characteristics of 70 cases. Am J Surg Pathol 2008;32:1727–35.

[13] Tournoy KG, Maddens S, Gosselin R, Van Maele G, van Meerbeeck JP, Kelles A. Integrated FDG-PET/CT does not make invasive staging of the intrathoracic lymph nodes in non-small cell lung cancer redundant: a prospective study. Thorax 2007;62:696–701.

[14] Lynch TJ, Bell DW, Sordella R, Gurubhagavatula S, Okimoto RA, Brannigan BW, et al. Activating mutations in the epidermal growth factor receptor underlying responsiveness of non-small-cell lung cancer to gefitinib. N Engl J Med 2004;350:2129–39.

Lung Cancer 68 (2010) 211–215

Contents lists available at ScienceDirect

Lung Cancer

journal homepage: www.elsevier.com/locate/lungcan

Combining transbronchial biopsy using endobronchial ultrasonography with a guide sheath and positron emission tomography for the diagnosis of small peripheral pulmonary lesions

Hidenori Mizugaki[a], Naofumi Shinagawa[a,*], Kakuko Kanegae[b], Noriyuki Yamada[a], Hajime Asahina[a], Eiki Kikuchi[a], Satoshi Oizumi[a], Nagara Tamaki[b], Masaharu Nishimura[a]

[a] First Department of Medicine, Hokkaido University School of Medicine, North 15, West 7, Kita-ku, Sapporo 060-8638, Japan
[b] Department of Nuclear Medicine, Hokkaido University Graduate School of Medicine, Sapporo 060-8638, Japan

ARTICLE INFO

Article history:
Received 28 February 2009
Received in revised form 11 May 2009
Accepted 8 June 2009

Keywords:
Peripheral pulmonary lesions
Endobronchial ultrasonography with a guide sheath
Transbronchial biopsy
Positron emission tomography with fluorodeoxyglucose
Standardized uptake value

ABSTRACT

To evaluate the combination of transbronchial biopsy (TBB) using endobronchial ultrasonography with a guide sheath (EBUS-GS) and positron emission tomography with fluorodeoxyglucose (FDG-PET) for the diagnosis of small peripheral pulmonary lesions (PPLs) ≤30 mm in mean diameter. A total of 74 PPLs (69.2%) were diagnosed by TBB using EBUS-GS with X-ray fluoroscopy. Diagnostic yield by FDG-PET was 78.5% for the 107 PPLs examined. Diagnostic yield with the combination of TBB using EBUS-GS and FDG-PET (90.7%) was significantly higher compared with that for each procedure alone. A significant increment in diagnostic yield with this combination was seen for PPLs >20 mm and ≤30 mm and for malignant lesions. Combination of TBB using EBUS-GS and FDG-PET is useful for the diagnosis of small PPLs.

1. Introduction

Various procedures have been developed to diagnose peripheral pulmonary lesions (PPLs). Transbronchial biopsy (TBB) procedures, which use a bronchoscope under fluoroscopic guidance, have been performed since the 1970s, with a diagnostic accuracy of 36–86% [1–5]. This diagnostic accuracy is influenced by lesion size. Schreiber and McCrory reported in a systematic review that the diagnostic accuracy for lesions <20 mm was 33% [1]. Other studies have found a diagnostic accuracy of 35–50% for benign lesions, lower than that for malignant lesions [2–5].

Currently, small-caliber radial-type ultrasound probes can be used for the clinical application of ultrasonography to examine tracheal–bronchial lesions. Endobronchial ultrasonography (EBUS) has been used for imaging guidance for TBB of PPLs [6,7]. Furthermore, Kurimoto et al. and our own preliminary study have shown the feasibility and effectiveness of TBB using EBUS with a guide sheath (EBUS-GS) [8,9], and several reports have since demonstrated the safety and efficacy of this method [10,11]. Nevertheless, the diagnostic yield of TBB using EBUS-GS in PPLs has been reported as 58–77% [8–13].

Recent advances in positron emission tomography with fluorodeoxyglucose (FDG-PET) have made significant contributions to differentiating between malignant and benign PPLs. Several reports have suggested that FDG-PET examinations reduce the number of patients with indeterminate PPLs undergoing unnecessary surgical biopsy [14–18]. However, FDG-PET is not always diagnostic, particularly for PPLs ≤30 mm in mean diameter. Malignant lesions such as well-differentiated adenocarcinoma and bronchiolo-alveolar carcinoma are frequently not identified on FDG-PET due to low glucose metabolism, while active inflammation sometimes shows positive FDG uptake due to high glucose metabolism [14–17].

These reports led us to the idea that the combination of TBB using EBUS-GS and FDG-PET might improve diagnostic yields for PPLs. The present study therefore evaluated a combination method for the diagnosis of small PPLs ≤30 mm in diameter.

2. Materials and methods

2.1. Patients

Medical records of 107 patients with 107 small PPLs (mean diameter, ≤30 mm) who underwent both TBB with EBUS-GS and

* Corresponding author. Tel.: +81 11 706 5911; fax: +81 11 706 7899.
E-mail address: naofu@med.hokudai.ac.jp (N. Shinagawa).

0169-5002/$ – see front matter © 2009 Elsevier Ireland Ltd. All rights reserved.
doi:10.1016/j.lungcan.2009.06.004

FDG-PET between August 2003 and March 2006 at Hokkaido University Hospital were retrospectively reviewed. PPLs were defined as lesions surrounded by pulmonary parenchyma that were endoscopically invisible (no evidence of endobronchial lesion, extrinsic compression, submucosal tumor, narrowing, inflammation or bleeding of the bronchus). All chest computed tomography (CT) images were reviewed, and mean diameters of PPLs were recorded. This study was approved by the Internal Review Board at our institution. All patients had provided written informed consent to undergo the procedures described below.

2.2. TBB using EBUS-GS

TBB using EBUS-GS was performed as described previously [8,9]. A 20-MHz mechanical radial-type probe (UM-S20-17R; Olympus Medical Systems, Tokyo, Japan) with an external diameter of 1.4 mm (1.4-mm probe) was most often used, and a 20-MHz mechanical radial-type probe (UM-S20-20R; Olympus) with an external diameter of 1.7 mm (1.7-mm probe) was used for PPLs assumed to be easily reached before bronchoscopy. The probe was connected to an EU-M30S endoscopic ultrasound system (Olympus). A flexible fiberoptic bronchoscope with a 2.0 mm diameter working channel (BF-P-260F; Olympus) and a guide sheath with an external diameter of 1.9 mm (B01-836-12; Olympus) were used for the 1.4-mm probe, and a flexible fiberoptic bronchoscope with a 2.8 mm ≤ diameter working channel (BF-1T30 and BF-1T260; Olympus) and a guide sheath with an external diameter of 2.7 mm (B01-836-13; Olympus) were used for the 1.7-mm probe. After the bronchoscope was inserted under local anesthesia as deeply as possible into the target bronchus under direct vision, an EBUS probe was inserted into the guide sheath, and the guide sheath-covered probe was then inserted through the bronchoscope working channel into the bronchus leading to the area suspected of containing the PPL. EBUS imaging and radiographic fluoroscopy were used to confirm that the probe and guide sheath had reached the PPL. When an EBUS image of the PPL was not obtained, the probe was removed from the guide sheath and a double-hinged curette was inserted into the guide sheath. The appropriate bronchus was then selected by manipulating the curette under fluoroscopic guidance. Once the bronchus was determined, the curette was removed from the guide sheath and the probe was again inserted into the guide sheath to obtain an EBUS image of the PPL. After locating the PPL on the EBUS image, the probe was removed from the guide sheath and the sheath was left in the PPL. Biopsy forceps and bronchial brushes were introduced via the guide sheath, and pathological and cytological specimens were obtained under fluoroscopic guidance. Bronchoscopic procedures were performed by eight pulmonary fellows, each with >4 years of training and experience in bronchoscopy.

When a definitive diagnosis was not obtained by TBB using EBUS-GS, the patient underwent other procedures (*e.g.*, video-assisted thoracoscopic surgery (VATS), percutaneous needle biopsy) or clinical and radiological follow-up examinations to confirm diagnosis of the PPL.

2.3. FDG-PET

FDG-PET was performed 60 min after injection of 4.5 MBq/kg body weight of fluorodeoxyglucose using an EXACT 47 scanner (Siemens, Munich, Germany). Patients had to fast for ≥6 h prior to FDG administration. Scanning itself encompassed an emission scan (2 min) and transmission (3 min) using rotating ^{68}Ge–^{68}Ga rod sources. Scans were reconstructed with the ordered subsets expectation maximization algorithm. FDG uptake was evaluated using the maximum standardized uptake value (SUV_{max}). FDG-PET was examined within 4 weeks before TBB using EBUS-GS.

Table 1
Established diagnosis in all 107 lesions.

Diagnosis	Lesions diagnosed by TBB using EBUS-GS/total lesions
Malignant	66/91
Lung cancer	59/80
Adenocarcinoma	33/44
Squamous cell carcinoma	12/17
Large cell carcinoma	1/4
Non-small cell carcinoma	6/7
Small cell carcinoma	7/8
Metastatic lung tumor	5/9
Lymphoma	1/1
Sarcoma	1/1
Benign	8/16
Non-tuberculous mycobacteriosis	3/4
Tuberculosis	1/1
Organizing pneumonia	2/2
Inflammatory change	0/4
Lung abscess	2/2
Others	0/3

2.4. Statistical analysis

The data that SUV_{max} and diagnostic yields by TBB with EBUS-GS alone and FDG-PET alone were analyzed using Pearson χ^2-test. The diagnostic yields by combining TBB using EBUS-GS and FDG-PET were analyzed using McNemar test. Statistical software (SPSS version 11.0.1; Chicago, IL) was used for all analyses. Statistical significance was established at the $p < 0.05$ level.

3. Results

3.1. Diagnostic yield by TBB using EBUS-GS

Mean (±standard deviation) diameter of the PPLs was 21.7 ± 6.1 mm (range, 9.5–30 mm). Of the 107 PPLs examined, a total of 92 PPLs (86.0%) were detected by EBUS. Definitive diagnosis was established for 74 PPLs (69.2%) by TBB using EBUS-GS (Table 1). Diagnostic yields for PPLs ≤20 mm and for PPLs >20 mm and ≤30 mm in mean diameter by TBB using EBUS-GS were 54.5% (24 of 44 PPLs) and 76.2% (48 of 63 PPLs), respectively. The diagnostic yield for PPLs ≤20 mm was significantly lower than that for PPLs >20 mm and ≤30 mm ($p < 0.05$). The diagnostic yield tended to be lower for benign disease (50.0%) than for malignant disease (72.5%), but this difference was not statistically significant.

3.2. Diagnostic yield by FDG-PET

In all PPLs, mean SUV_{max} for FDG-PET was 4.2 ± 2.9. A significant difference in SUV_{max} was seen between malignant disease (4.5 ± 3.0) and benign disease (2.5 ± 1.6; $p < 0.01$). With malignant disease, a significant difference in SUV_{max} was seen between PPLs ≤20 mm (2.9 ± 1.4) and PPLs >20 mm and ≤30 mm (5.5 ± 3.2; $p < 0.01$). Conversely, with benign disease, no significant differences were seen according to tumor size (Table 2).

To determine a cut-off value of SUV_{max} for diagnosing pulmonary malignancy with FDG-PET, we analyzed the receiver operating characteristics (ROC) curve of SUV_{max} in all PPLs. The ROC

Table 2
Mean maximum standard uptake for FDG-PET.

	≤20 mm	>20 mm and ≤30 mm	Total
Malignant	2.9 ± 1.4	5.5 ± 3.2	4.5 ± 3.0
Benign	2.5 ± 1.6	2.5 ± 1.8	2.5 ± 1.6
Total	2.8 ± 1.5	5.2 ± 3.2	4.2 ± 2.9

Values represent mean ± standard deviation.

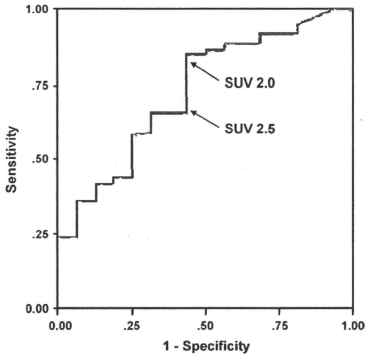

Fig. 1. Receiver operating characteristics (ROC) curve of SUV_{max} in all PPLs. The ROC curve showed that the cut-off value of 2.0 offered the highest sensitivity and specificity.

curve showed that a cut-off value of 2.0 would provide the highest sensitivity and specificity (Fig. 1). We then selected a cut-off value of 2.0 of SUV_{max} for the following analysis in this study.

When using this criterion, diagnostic yield was 78.5% for the 107 PPLs examined. Diagnostic yields by FDG-PET of PPLs ≤20 mm and PPLs >20 mm and ≤30 mm were 70.5% (31 of 44 PPLs) and 84.1% (53 of 63 PPLs), respectively. Diagnostic yield was significantly lower for PPLs ≤20 mm than for PPLs >20 mm and ≤30 mm ($p < 0.01$). Diagnostic yield was also significantly lower for benign disease (56.3%) than for malignant disease (82.4%; $p < 0.01$).

3.3. Diagnostic yield with combination of TBB using EBUS-GS and FDG-PET

Next, the diagnostic yield by combining TBB using EBUS-GS and FDG-PET was evaluated (Table 3; results for each method are also shown). Diagnostic yield with the combination of TBB using EBUS-GS and FDG-PET was 90.7% for the 107 PPLs examined. In addition, sensitivity, specificity, positive predictive value, and negative predictive value for combination of TBB using EBUS-GS and FDG-PET were 94.5, 68.8, 94.5, and 68.8%, respectively. According to size, diagnostic yield for PPLs >20 mm and ≤30 mm in mean diameter reached 96.8%, while diagnostic yield for PPLs ≤20 mm was 81.8%. When restricted to malignant diseases, diagnostic yield with the combination of techniques (94.5%) was still significantly higher than those for each procedure alone (72.5% by TBB with EBUS-GS alone; 82.4% by FDG-PET alone). Diagnostic yield for malignant diseases with PPLs >20 mm and ≤30 mm using the combination method reached 100%. Conversely, no significant differences in diagnostic yields were seen for benign disease, although diagnostic yield with the combination method (68.8%) tended to be higher than those for each procedure alone (50.0% for EBUS-GS alone; 56.3% for FDG-PET alone).

3.4. Non-diagnostic lesions by both TBB using EBUS-GS and FDG-PET

Even after combining TBB using EBUS-GS with FDG-PET, diagnostic yields did not reach 100%, and 10 PPLs were not diagnosed even by the combination method. These 10 PPLs comprised five malignant lesions (adenocarcinoma, $n = 3$; large cell carcinoma, $n = 1$; metastasis of renal cell carcinoma, $n = 1$) and five benign lesions (pneumonia, $n = 3$; radiation pneumonitis, $n = 1$; and pneumoconiosis, $n = 1$). Six PPLs (five malignant lesions and one pneumoconiosis lesion) were diagnosed by VATS, 1 PPL (radiation pneumonia) by repeated TBB using EBUS-GS, and 3 PPLs (pneumonia) by follow-up examinations. Mean diameter of these PPLs was 16.4 mm. Mean SUV_{max} for the five malignant PPLs and five benign PPLs were 1.39 and 3.53, respectively.

3.5. Representative cases

The first case involved a 61-year-old man presenting with a small PPL 10 mm in mean diameter in the left segment 4 (Fig. 2). On FDG-PET, slight FDG uptake was observed in the left upper lobe (SUV_{max}, 1.45). The PPL was diagnosed as lung adenocarcinoma. This case was representative of a false-negative finding on FDG-PET.

The second case involved a 74-year-old man with chronic obstructive pulmonary disease (COPD) presenting with a small PPL of 15 mm in mean diameter in segment 6 of the right lung (Fig. 3). On FDG-PET, high uptake was seen in the right lower lobe (SUV_{max}, 4.52). TBB using EBUS-GS was not diagnostic, while partial resection by VATS revealed squamous cell carcinoma. This case was representative of cases in which FDG-PET was useful for the diagnosis of malignant disease, but TBB with EBUS-GS was not.

4. Discussion

The present study combined TBB using EBUS-GS with FDG-PET for the diagnosis of small PPLs ≤30 mm in mean diameter. This is the first report that shows the usefulness of combination of EBUS-GS and FDG-PET for pulmonary peripheral lesions. As a result, diagnostic yield with this combination was >90%, significantly higher than with each procedure alone. We have provided novel, important evidence that the combination of TBB using EBUS-GS and FDG-PET is useful in the diagnosis of small PPLs. Chhajed et al. have already reported the usefulness of combining TBB with FDG-PET in the diagnosis of small PPLs ≤30 mm in mean diameter [19]. However, they used conventional bronchoscopy, and the diagnostic yield of bronchoscopy was 53%, including 8% for endobronchial lesions. As TBB with EBUS-GS is obviously superior to conventional bronchoscopy, particularly for the diagnosis of smaller PPLs [8–13], our results will

Table 3
Diagnostic yields of combination TBB using EBUS-GS and FDG-PET.

	≤20 mm			>20 mm and ≤30 mm			Total		
	EBUS-GS	FDG-PET	EBUS-GS/FDG-PET	EBUS-GS	FDG-PET	EBUS-GS/FDG-PET	EBUS-GS	FDG-PET	EBUS-GS/FDG-PET
Malignant	57.1%	74.3%	85.7%* ($n = 35$)	78.6%	87.5%	100%† ($n = 56$)	72.5%	82.4%	94.5%‡ ($n = 91$)
Benign	44.4%	55.6%	66.7% ($n = 9$)	57.1%	57.1%	71.4% ($n = 7$)	50.0%	56.3%	68.8% ($n = 16$)
Total	54.5%	70.5%	81.8%* ($n = 44$)	76.2%	84.1%	96.8%† ($n = 63$)	69.2%	78.5%	90.7%‡ ($n = 107$)

Data were analyzed using the McNemar test.
* $p < 0.01$ compared to EBUS-GS.
† $p < 0.01$ compared to EBUS-GS and $p < 0.05$ compared to FDG-PET.
‡ $p < 0.01$ compared to EBUS-GS and FDG-PET.

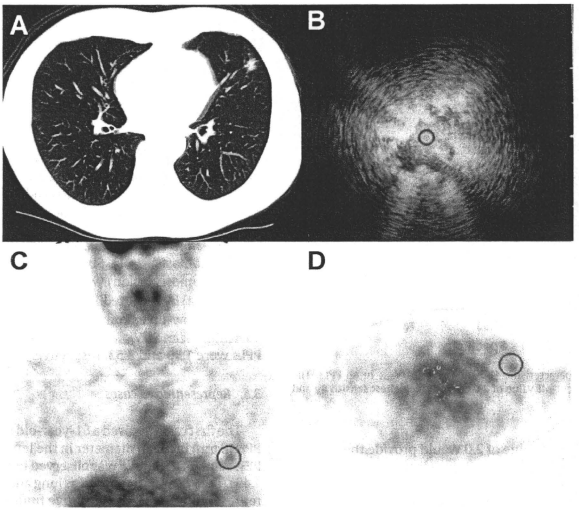

Fig. 2. Images from a 61-year-old man with lung adenocarcinoma showing false-negative findings on FDG-PET. (A) On chest CT, a small PPL 10 mm in mean diameter is seen in segment 4 of the left lung. (B) EBUS revealing the PPL, which was diagnosed as adenocarcinoma by TBB using EBUS-GS. (C and D) On FDG-PET, transverse and coronal scans demonstrate slight FDG uptake in the left upper lobe (SUV_{max}, 1.45).

contribute to the development of diagnostic procedures for small PPLs.

Some previous reports have used a cut-off SUV_{max} of 2.5 [15,19], but no obvious validation has been provided for this value, particularly for small PPLs ≤30 mm in mean diameter. In the present study, we selected a cut-off SUV_{max} of 2.0, as the ROC curve of SUV_{max} for all PPLs showed that this value offered higher sensitivity and specificity than 2.5. Bryant and Cerfolio reported that in small PPLs ≤25 mm, 24% of nodules with SUV_{max} ≤2.5 were malignant [20]. When using a cut-off of 2.0, diagnostic yield by FDG-PET was 78.5% for the 107 PPLs examined (82.4% for malignant, 56.3% for benign), similar to the findings of previous studies [21]. Determining the optimal cut-off value for FDG-PET in each study using reliable methods such as ROC curves is important.

However, FDG-PET is not always diagnostic, particularly for small PPLs. Small malignant lesions ≤30 mm in mean diameter could show lower FDG uptake than larger malignant tumors, due to partial-volume effects [22]. Malignant lesions such as well-differentiated adenocarcinoma and bronchiolo-alveolar carcinoma are frequently missed by FDG-PET due to low glucose metabolism [12–15,17,18]. In this study, the 44 adenocarcinomas included 14 PPLs that were false-negative on FDG-PET, and pathological review showed that these 14 PPLs comprised 11 well-differentiated adenocarcinomas and 3 bronchiolo-alveolar carcinomas. Of note is the fact that the 11 adenocarcinomas were successfully diagnosed by TBB using EBUS-GS, even without positive FDG-PET findings.

In contrast, there are false-positives in FDG-PET for detecting pulmonary malignancy. Physicians always have to consider the possibility that FDG-PET findings are false-positive as malignant

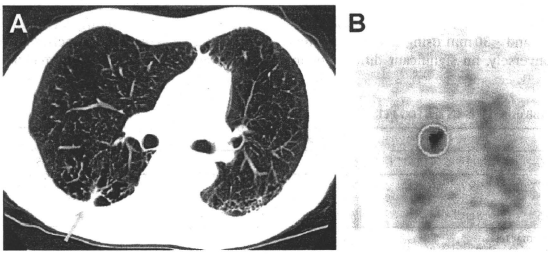

Fig. 3. Images from a 74-year-old man with COPD and squamous cell carcinoma of the lung showing positive findings on FDG-PET. (A) On chest CT, a small PPL 15 mm in mean diameter is seen in segment 6 of the right lung. (B) On FDG-PET, coronal scan demonstrates higher FDG uptake in the right lower lobe (SUV_{max}, 4.52).

lesions, especially in pulmonary benign diseases such as sarcoidosis or active inflammatory changes. In the case, again, EBUS-GS is useful; definitive identification can be accomplished by TBB with EBUS-GS, referring to clinical features or laboratory data. Subsequently, patients are able to receive proper treatment.

Even after combining TBB using EBUS-GS with FDG-PET, diagnostic yield did not reach 100%. The increment in diagnostic yield with the combination method was more apparent with PPLs >20 mm and ≤30 mm and with malignant lesions. Ten PPLs remained undiagnosed even with the combination method. These 10 PPLs comprised five malignant lesions and five benign lesions, and mean diameter of these PPLs was 16.4 mm. The limitations of the combination method must be kept in mind, particularly in small PPLs ≤20 mm. The present study encountered no complications associated with TBB using EBUS-GS or FDG-PET that required hospitalization.

5. Conclusion

In conclusion, based on our retrospective analysis, the combination of TBB with EBUS-GS and FDG-PET increased diagnostic yield to >90%, representing a useful method for the diagnosis of small PPLs ≤30 mm. In cases where neither TBB using EBUS-GS nor FDG-PET is diagnostic, the combination strategy supports the decision of the physician as to whether more invasive procedures or clinical and radiological follow-up are required for the management of PPLs.

Conflict of interest statement

The authors have no conflict of interest to declare.

Acknowledgements

We gratefully acknowledge the outstanding support of Dr. Koichi Yamazaki, former Associate Professor of the First Department of Medicine at Hokkaido University School of Medicine.

References

[1] Schreiber G, McCrory DC. Performance characteristics of different modalities for diagnosis of suspected lung cancer: summary of published evidence. Chest 2003;123:115s–28s.
[2] Baaklini WA, Reinoso MA, Gorin AB, Sharafkaneh A, Manian P. Diagnostic yield of fiberoptic bronchoscopy in evaluating solitary pulmonary nodules. Chest 2000;117:1049–54.
[3] Chechani V. Bronchoscopic diagnosis of solitary pulmonary nodules and lung masses in the absence of endobronchial abnormality. Chest 1996;109:620–5.
[4] Gasparini S, Ferretti M, Secchi EB, Baldelli S, Zuccatosta L, Gusella P. Integration of transbronchial and percutaneous approach in the diagnosis of peripheral pulmonary nodules or masses: experience with 1,027 consecutive cases. Chest 1995;108:131–7.
[5] Radke JR, Conway WA, Eyler WR, Kvale PA. Diagnostic accuracy in peripheral lung lesions. Factors predicting success with flexible fiberoptic bronchoscopy. Chest 1979;76:176–9.
[6] Herth FJF, Ernst A, Becker HD. Endobronchial ultrasound-guided transbronchial lung biopsy in solitary pulmonary nodules and peripheral lesions. Eur Respir J 2002;20:972–4.
[7] Paone G, Nicastri E, Lucantoni G, Iacono RD, Battistoni P, D'Angeli AL, et al. Endobronchial ultrasound-driven biopsy in the diagnosis of peripheral lung lesions. Chest 2005;128:3551–7.
[8] Kurimoto N, Miyazawa T, Okimasa S, Maeda A, Oiwa H, Miyazu Y, et al. Endobronchial ultrasonography using a guide sheath increases the ability to diagnose peripheral pulmonary lesions endoscopically. Chest 2004;126:959–65.
[9] Kikuchi E, Yamazaki K, Sukoh N, Kikuchi J, Asahina H, Imura M, et al. Endobronchial ultrasonography with guide-sheath for peripheral pulmonary lesions. Eur Respir J 2004;24:533–7.
[10] Shirakawa T, Imamura F, Hamamoto J, Honda I, Fukushima K, Sugimoto M, et al. Usefulness of endobronchial ultrasonography for transbronchial lung biopsies of peripheral lung lesions. Respiration 2004;71:260–8.
[11] Herth FJF, Eberhardt R, Becker HD, Ernst A. Endobronchial ultrasound-guided transbronchial lung biopsy in fluoroscopically invisible solitary pulmonary nodules: prospective trial. Chest 2006;129:147–50.
[12] Asahina H, Yamazaki K, Onodera Y, Kikuchi E, Shinagawa N, Asano F, et al. Transbronchial biopsy using endobronchial ultrasonography with a guide sheath and virtual bronchoscopic navigation. Chest 2005;128:1761–5.
[13] Yamada N, Yamazaki K, Kurimoto N, Asahina H, Kikuchi E, Shinagawa N, et al. Factors related to diagnostic yield of transbronchial biopsy using endobronchial ultrasonography with a guide sheath in small peripheral pulmonary lesions. Chest 2007;132:603–8.
[14] Scott WJ, Schwabe JL, Gupta NC, Dewan NA, Reeb SD, Sugimoto JT. Positron emission tomography of lung tumors and mediastinal lymph nodes using [^{18}F] fluorodeoxyglucose. Ann Thorac Surg 1994;58:698–703.
[15] Patz EF, Lowe VJ, Hoffman JM, Paine SS, Burrowes P, Coleman RE, et al. Focal pulmonary abnormalities: evaluation with F-18 fluorodeoxyglucose PET scanning. Radiology 1993;188:487–90.
[16] Gupta NC, Maloof J, Gunel E. Probability of malignancy in solitary pulmonary nodules using fluorine-18-FDG and PET. J Nucl Med 1996;37:943–8.
[17] Gupta NC, Gill H, Graeber G, Bishop H, Hurst J, Stephens T. Dynamic positron emission tomography with F-18 fluorodeoxyglucose imaging in differentiation of benign from malignant lung/mediastinal lesions. Chest 1998;114:1105–11.
[18] Gambhir SS, Shepherd JE, Shah BD, Hart E, Hoh CK, Valk PE, et al. Analytical decision model for the cost-effectiveness management of solitary pulmonary nodules. J Clin Oncol 1998;16:2113–25.
[19] Chhajed PN, Bernasconi M, Gambazzi F, Bubendorf L, Rasch H, Kneifel S, et al. Combining bronchoscopy and positron emission tomography for the diagnosis of the small pulmonary nodule < or = 3 cm. Chest 2005;128:3558–64.
[20] Bryant AS, Cerfolio RJ. The maximum standardized uptake values on integrated FDG-PET/CT is useful in differentiating benign from malignant pulmonary nodules. Ann Thorac Surg 2006;82:1016–20.
[21] Farrell MA, McAdams HP, Herndorn JE, Patz EF. Non-small cell lung cancer: FDG PET for nodal staging in patients with stage I disease. Radiology 2000;215:886–90.
[22] Key Jr JW. SUV: standard uptake or silly useless value? J Nucl Med 1995;36:1836–9.

Cancer Immunol Immunother (2010) 59:1543–1549
DOI 10.1007/s00262-010-0881-6

ORIGINAL ARTICLE

$CD8^+$ tumor-infiltrating lymphocytes predict favorable prognosis in malignant pleural mesothelioma after resection

Noriyuki Yamada · Satoshi Oizumi · Eiki Kikuchi · Naofumi Shinagawa · Jun Konishi-Sakakibara · Atsushi Ishimine · Keisuke Aoe · Kenichi Gemba · Takumi Kishimoto · Toshihiko Torigoe · Masaharu Nishimura

Received: 21 March 2010 / Accepted: 7 June 2010 / Published online: 22 June 2010

Abstract Defects in human leukocyte antigen (HLA) class I expression may allow tumor cells to escape immune recognition. T cell infiltration is associated with a good prognosis in many cancers. However, the role of HLA class I expression and tumor-infiltrating lymphocytes (TILs) in malignant pleural mesothelioma (MPM) has not been fully analyzed. In the present study, we investigated the immune profiles and conducted outcome analyses of MPM patients. HLA class I expression and TILs ($CD4^+$, $CD8^+$, and NK cells) were detected by immunohistochemistry in a series of 44 MPM cases. To detect HLA class I expression, specimens were stained with the anti-pan HLA class I monoclonal antibody EMR8-5. The expression of HLA class I was positive in all patients. There was no case that showed negative HLA class I expression. The density of $CD4^+$ and $CD8^+$ TILs were strongly correlated ($R = 0.76$, $p < 0.001$). A high density of $CD8^+$ TILs was a significantly better prognostic factor for the survival of patients with extrapleural pneumonectomy ($p < 0.05$). Multivariate analysis revealed that a high density of $CD8^+$ TILs is an independent prognostic factor for patients who underwent extrapleural pneumonectomy. The presence of intratumoral $CD8^+$ T cells was correlated with an improved clinical outcome, raising the possibility that $CD8^+$ T cells might play a pivotal role in the antitumor immune response against MPMs. Thus, the stimulation of $CD8^+$ lymphocytes might be an efficacious immunotherapy for MPM patients.

Keywords Malignant pleural mesothelioma · HLA class I · Tumor-infiltrating lymphocytes (TIL) · Immunohistochemistry · Immunotherapy

N. Yamada · S. Oizumi (✉) · E. Kikuchi · N. Shinagawa · J. Konishi-Sakakibara · M. Nishimura
First Department of Medicine, Hokkaido University School of Medicine, North 15, West 7, Kita-ku, Sapporo 060-8638, Japan
e-mail: soizumi@med.hokudai.ac.jp

A. Ishimine
Department of Internal Medicine, Kin-Ikyo Chuo Hospital, Sapporo, Japan

K. Aoe
Department of Medical Oncology and Clinical Research, NHO Yamaguchi-Ube Medical Center, Ube, Japan

K. Gemba · T. Kishimoto
Department of Respiratory Medicine, Okayama Rosai Hospital, Okayama, Japan

T. Torigoe
Department of Pathology 1, Sapporo Medical University School of Medicine, Sapporo, Japan

Abbreviations

HLA	Human leukocyte antigen
TILs	Tumor-infiltrating lymphocytes
MPM	Malignant pleural mesothelioma

Introduction

The incidence of malignant pleural mesothelioma (MPM) is increasing worldwide as a result of widespread workplace exposure to asbestos that occurred in the past [1–3]. It has been predicted that 250,000 deaths in Europe and 103,000 deaths in Japan will be caused by MPM over the next 40 years [4]. MPM is a highly aggressive tumor. It has a poor prognosis, despite treatment efforts such as

extrapleural pneumonectomy [5], the new chemotherapeutic agent pemetrexed [6], and postoperative intensity-modulated radiotherapy [7]. To improve the prognosis of MPM, more effective therapeutic strategies, including the development of immunotherapy, are required. However, there is still uncertainty about the immune profiles in MPM, which is not an epithelial tumor.

Human leukocyte antigen (HLA) class I antigens are expressed on the surface of most human cells and present specific antigens. $CD8^+$ cytotoxic T lymphocytes can induce tumor killing upon direct recognition of tumor-specific antigens presented on HLA class I antigens on the surface of tumor cells.

Tumor-infiltrating lymphocytes (TILs) recognize tumor-specific antigens, thereby playing an important role in immune defense. In several cancers, the presence of TILs and the expression of HLA class I antigen are associated with prognosis [8–13]. In MPM, however, the role of TILs and HLA class I antigen is not well understood.

Here, we performed immunohistochemical assessment of HLA class I expression and TILs in patients with MPM. We also evaluated whether there is an association between immune profiles and clinical outcomes.

Materials and methods

Patients and specimens

Paraffin-embedded tumor specimens were obtained from 44 patients diagnosed with MPM between May 1997 and January 2008 in four institutes. This study was approved by the institutional review boards of each institute, and all patients provided written informed consent. Histopathological diagnoses were established by pathologists from each institute, and clinicopathological information was collected from patient charts. The TNM stage was based on the International Mesothelioma Interest Group classification [14]. A survival analysis of patients who underwent either curative extrapleural pneumonectomy or chemotherapy was conducted. Overall survival was defined as the time from the date of surgery or initiation of chemotherapy to death from any cause.

Immunohistochemistry

The following primary antibodies were used: anti-human HLA class I A, B, C (clone EMR8-5, Hokudo, Sapporo, Japan; 1:100 dilution), anti-human CD4 (clone 1F6, Novocastra, Newcastle, UK; 1:20 dilution), anti-human CD8 (clone C8/144b, DAKO, Glostrup, Denmark; 1:50 dilution) and anti-human CD56 (clone 1B6, Novocastra; 1:50 dilution). Tumor specimens were cut into sequential 5-μm-thick sections and deparaffinized by xylene and rehydrated by ethanol. Antigen retrieval was performed by autoclave heating at 121°C for 20 min in 10 nM citrate buffer (pH 6.0) for anti-human HLA class I and Tris–EDTA buffer (pH 9.0) for anti-human CD4, anti-human CD8, and anti-human CD56. Endogenous peroxidase activity was blocked with 0.3% hydrogen peroxide for anti-human CD4 and 3% hydrogen peroxide for anti-human HLA class I, anti-human CD8 and anti-human CD56. Then, tissue slides were incubated at room temperature for 1 h with anti-human HLA class I, anti-human CD4, or anti-human CD56; or, alternatively, the slides were kept at 4°C overnight with anti-human CD8. After incubation with the primary antibody, the streptavidin–biotin complex (SimpleStain MAX-PO kit, Nichirei, Tokyo, Japan) was used, followed by reaction with 3,3′-diaminobenzidine tetrahydrochloride–hydrogen peroxide as a chromogen and counterstaining with hematoxylin solution.

Evaluation of HLA class I and TILs

Expression of HLA class I was assessed by two investigators (N.Y. and E.K.) who were not informed of the patients' clinicopathological data. To evaluate HLA class I, the percentage of tumor cells with immunoreactivity on their membranes was calculated for at least five high-power (400×) fields. Average in the percentage of HLA class I positive cells were defined as frequency of HLA class I for each case.

To examine TILs, the number of cells per microscopic field (400×) with immunoreactivity to CD4, CD8 and CD56 were counted in five independent areas with the most abundant immunoreactive cells. We defined the average value of the five highest numbers in the slide as the number of TILs for each case. For analysis of association with prognosis, the patients were divided into two groups by the median number as the cutoff.

Statistical analysis

Data were analyzed with Pearson's chi-squared test. Densities of TILs were compared with the Student's t test. Survival probabilities were studied by the Kaplan–Meier method, and differences in survival time between patient subgroups were analyzed with a log-rank test. Uni- and multi-variate analyses were performed with the Cox proportional hazards model to estimate correlations between the immunohistological factors and overall survival. Statistical software (SPSS version 11.0.1; Chicago, IL) was utilized for all analyses. Statistical significance was established at the $p < 0.05$ level, and all analyses were two-sided.